Title: Chlorellestadite, Ca5(SiO4)1.5(SO4)1.5Cl, a new ellestadite- group mineral from the Shadil-Khokh volcano, South Ossetia

Author: Dorota Środek, Irina O. Galuskina, Evgeny Galuskin, Mateusz Dulski, Maria Książek, Joachim Kusz i in.

Citation style: Środek Dorota, Galuskina Irina O., Galuskin Evgeny, Dulski Mateusz, Książek Maria, Kusz Joachim i in. (2018). Chlorellestadite, Ca5(SiO4)1.5(SO4)1.5Cl, a new ellestadite- group mineral from the Shadil-Khokh volcano, South Ossetia. "Mineralogy and Petrology" (Vol. 112, iss. 5 (2018), s. 743-752), doi 10.1007/s00710-018-0571-1

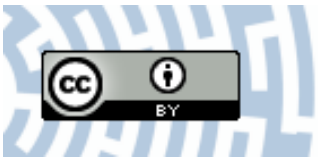

Mineralogy and Petrology (2018) 112:743–752
https://doi.org/10.1007/s00710-018-0571-1

ORIGINAL PAPER

Chlorellestadite, $Ca_5(SiO_4)_{1.5}(SO_4)_{1.5}Cl$, a new ellestadite- group mineral from the Shadil-Khokh volcano, South Ossetia

Dorota Środek[1] · Irina O. Galuskina[1] · Evgeny Galuskin[1] · Mateusz Dulski[2,3] · Maria Książek[4] · Joachim Kusz[4] · Viktor Gazeev[5]

Received: 7 September 2017 / Accepted: 2 April 2018 / Published online: 3 May 2018

Abstract

Chlorellestadite (IMA2017–013), ideally $Ca_5(SiO_4)_{1.5}(SO_4)_{1.5}Cl$, the Cl-end member of the ellestadite group was discovered in a calcium-silicate xenolith in rhyodacite lava from the Shadil Khokh volcano, Greater Caucasus, South Ossetia. Chlorellestadite forms white, tinged with blue or green, elongate crystals up to 0.2–0.3 mm in length. Associated minerals include spurrite, larnite, chlormayenite, rondorfite, srebrodolskite, jasmundite and oldhamite. The empirical crystal chemical formula of the holotype specimen is $Ca_{4.99}Na_{0.01}(SiO_4)_{1.51}(SO_4)_{1.46}(PO_4)_{0.03}(Cl_{0.61}OH_{0.21}F_{0.11})_{\Sigma 0.93}$. Unit-cell parameters of chlorellestadite are: $P6_3/m$, $a = 9.6002(2)$, $c = 6.8692(2)$ Å, $V = 548.27(3)$Å^3, $Z = 2$. Chlorellestadite has a Mohs hardness of 4–4.5 and a calculated density of 3.091 g/cm^3. The cleavage is indistinct, and the mineral shows irregular fracture. The Raman spectrum of chlorellestadite is similar to the spectra of other ellestadite group minerals, with main bands located at 267 cm^{-1} (Ca–O vibrations), and between 471 and 630 cm^{-1} (SiO_4^{4-} and SO_4^{2-} bending vibrations) and 850–1150 cm^{-1} (SiO_4^{4-} and SO_4^{2-} stretching modes). Chlorellestadite forms in xenoliths of calcium-silicate composition when they are exposed to Cl-bearing volcanic exhalations at about 1000 °C under low pressure conditions.

Keywords Chlorellestadite · New mineral · Crystal structure · Raman · Shadil Khokh volcano · South Ossetia

Introduction

Chlorellestadite, ideally $Ca_5(SiO_4)_{1.5}(SO_4)_{1.5}Cl$, was found in an altered calcium-silicate xenolith enclosed in rhyodacite lava from the Shadil Khokh volcano, Greater Caucasus, South Ossetia. It is a new mineral of the ellestadite group consisting of silicate-sulfate apatites (Rouse and Dunn 1982), belonging to the apatite supergroup (Pasero et al. 2010). To date, the ellestadite group has been known to contain only three confirmed minerals:

- fluorellestadite $Ca_5(SiO_4)_{1.5}(SO_4)_{1.5}F$,
- hydroxylellestadite $Ca_5(SiO_4)_{1.5}(SO_4)_{1.5}(OH)$, and
- mattheddleite $Pb_5(SiO_4)_{1.5}(SO_4)_{1.5}Cl$.

The natural existence of chlorellestadite was long doubted mainly due to the lack of credible analyses (Rouse and Dunn 1982) and its species name was thus proposed discredited (Pasero et al 2010, p. 175) Now, the confirmed Cl-member of the fluorellestadite-hydroxylellestadite series supplements this group. All Ca-members of the ellestadite group have comparable optical and physical properties (Table 1), whereas matthedlleite is quite different.

"Chlorellestadite" was first described from Crestmore, California, USA (McConnell 1937). Further studies revealed errors in his crystal chemical formula calculations. As later assessment has shown that hydroxyl dominates over chlorine

Editorial handling: M. A.T.M. Broekmans

✉ Dorota Środek
srodek.dorota@gmail.com

[1] Faculty of Earth Sciences, Department of Geochemistry, Mineralogy and Petrography, University of Silesia, Będzińska 60, 41-200 Sosnowiec, Poland

[2] Silesian Center for Education and Interdisciplinary Research, Institute of Material Science, 75 Pułku Piechoty 1a, 41-500 Chorzów, Poland

[3] Institute of Material Science, University of Silesia, 75 Pułku Piechoty 1a, 41-500 Chorzów, Poland

[4] Institute of Physics, University of Silesia, Uniwersytecka 4, 40-007 Katowice, Poland

[5] Institute of Geology of Ore Deposits, Petrography, Mineralogy & Geochemistry (IGEM) RAS, Staromonetny 35, 119017 Moscow, Russia

Table 1 Comparison physical properties of the ellestadite group minerals

mineral species	Fluorellestadite (Chesnokov et al. 1987)	Hydroxylellestadite (Harada et al. 1971)	Chlorellestadite	Mattheddleite (Livingstone et al. 1987)
end-member formula	$Ca_5(SiO_4)_{1.5}(SO_4)_{1.5}F$	$Ca_5(SiO_4)_{1.5}(SO_4)_{1.5}(OH)$	$Ca_5(SiO_4)_{1.5}(SO_4)_{1.5}Cl$	$Pb_5(SiO_4)_{1.5}(SO_4)_{1.5}Cl$
crystal data	$P6_3/m$ $a = 9.485$ (2) Å $c = 6.916$ (2) Å $V = 538.8$ Å^3	$P6_3/m$ $a = 9.496$ (2) Å $c = 6.920$ (2) Å $V = 540.4$ Å^3	$P6_3/m$ a = 9.6002 (2) Å c = 6.8692 (2) Å V = 548.27 (3) Å^3	$P6_3/m$ a = 10.0056 (6) Å c = 7.4960 (9) Å V = 649.9 (1) Å^3
density	3.10 g/cm^3	3.11 g/cm^3	3.09 g/cm^3	6.96 g/cm^3
optical properties	(−) ω = 1.658 ε = 1.632, Δ = 0.006	(−) ω = 1.654, ε = 1.650, Δ = 0.004	(−) ω = 1.664(3), ε = 1.659(3), Δ = 0.005	(−) ω = 2.017, ε = 1.999, Δ = 0.018
strong lines and intensities in diffraction pattern, d_{hkl}	1.852 (8), 1.729 (7), 1.766 (6), 1.463 (6), 1.904 (5), 1.819 (5), 1.792 (5), 1.486 (5)	2.839 (100), 2.739 (60), 2.655 (45), 2.801 (44), 1.853 (43), 3.462 (40), 1.484 (20)	2.858 (100), 2.771 (99), 2.793 (90), 2.858 (41), 3.435 (38), 1.851 (23)	2.988 (100), 4.32 (40), 4.13 (40), 2.877 (40), 3.26 (30)

and fluorine in ellestadite from Crestmore, this mineral is hydroxylellestadite (Rouse and Dunn 1982). Synthetic chlorellestadite was first reported by Pliego-Cuervo and Glasser (1977). Later, chlorellestadite was described as an intermediate high-temperature phase in Portland clinker (Chen and Fang 1989; Saint-Jean and Hansen 2005) and was used as a synthetic phase for production of new technological materials (Fang et al. 2011, 2014). It merits noting that Cl-bearing ellestadite was reported from burned coal spoil-heaps near Brno, Czech Republic (Sejkora et al. 1999) but, to date, Cl-dominant ellestadite had not otherwise been found in natural rocks.

Recent study of Cl-bearing minerals in altered xenoliths from the Shadil-Khokh volcano revealed a Cl-dominant member of the ellestadite group. This phase was investigated and the new mineral species chlorellestadite (IMA2017–013) was approved by the IMA Commission for New Minerals, Nomenclature and Classification – CNMNC in 2017.

The altered xenolith in which chlorellestadite was found is a pyrometamorphic rock formed under sanidinite facies (larnite sub-facies) conditions at temperature above 750 °C and low, near-ambient pressure. A metasomatic alteration of primary silicate-carbonate xenolith affected by fluid and gas of volcanic origin, and enriched with chlorine, is responsible for the formation of chlorellestadite.

The type material of chlorellestadite is deposited in the mineralogical collection of the Fersman Mineralogical Museum, Leninskiy pr., 18/k2, 115,162 Moscow, Russia, under catalogue number 4975/1.

Methods of investigation

Chlorellestadite was initially identified as an unknown mineral by electron scanning microscope on polished sections prepared from several fist-sized xenolith samples that were collected during fieldwork in Summer 2012.

The crystal morphology and mineral assemblage of the chlorellestadite were assessed using an Olympus BX51 optical petrographic microscope, and a scanning electron microscope – SEM Phenom XL (Faculty of Earth Sciences, University of Silesia, Poland). Several locations suitable for analysis in an electron-probe micro-analyzer – EPMA were selected from a number of polished sections. A monomineralic chlorellestadite grain for single-crystal X-ray diffraction was extracted from a polished section using a preparation needle.

The chemical composition of the chlorellestadite was determined using a CAMECA SX100 equipped with one EDS detector and five WDS detectors with LIF, PET and TAP crystals located at the Institute of Geochemistry, Mineralogy and Petrology, University of Warsaw, Poland. The EPMA instrument was operated at ~$3{\cdot}10^{-6}$ Torr, 15 kV acceleration voltage, 10 nA beam current (measured with a Faraday cup) and 5–8 μm diameter as confirmed by the beam imprint on the specimen. The beam was intentionally defocused to reduce migration of, in particular, Na, F, and Cl (see e.g., Le Roy and Roinel 1983; Morgan and London 1996). The instrument was internally calibrated against the following mineral standards: wollastonite – Ca, Si; baryte – S; fluorapatite – P, F; albite – Na; tugtupite – Cl, and all elements were measured on their $K\alpha$ lines. Contents of other elements are lower detection limits. Raw data were ZAF-corrected using the PAP-protocol (Pouchou and Pichoir 1985), and element contents were converted to oxides assuming stoichiometry. Main oxide contents in wt% were recalculated into atoms per formula unit based on 8 cations and 12O (Table 2).

Single-crystal X-ray diffraction on an extracted chlorellestadite grain approximately 20 × 20 × 20 μm in size was carried out using a SuperNova Dual diffractometer with a

Table 2 Chemical composition of chlorellestadite (mean 11)

	Wt.%	Range	Stand. Dev.
CaO	54.43	54.71–57.51	0.37
Na_2O	0.07	0.00–0.18	0.05
SO_3	22.72	22.90–23.70	0.22
SiO_2	17.67	17.64–18.95	0.19
P_2O_5	0.44	0.10–0.99	0.03
Cl	4.23	4.03–4.89	0.18
F	0.40	0.10–0.70	0.16
OH*	0.49	0.38–0.74	
	100.45		
-O = (F, Cl)	1.12		
	99.33		

*- water was calculated on the basis of charge balance

mirror monochromator (MoKα, λ = 0.71073 Å) and an Atlas CCD detector (Agilent Technologies), located at the Institute of Physics, University of Silesia, Poland. The structure of synthetic chlorellestadite (Saint-Jean and Hansen 2005) was taken as the initial model. Subsequently, the structure of the natural chlorellestadite was refined using the program SHELX-2014/6 (Sheldrick 2015) to $R1 = 3.56\%$. Refinement including anisotropic atom displacement-parameters (excluding anions in in channel sites) was carried out with neutral atom scattering-factors (see Table 3, 4, 5 and 6).

Raman spectra of the chlorellestadite were recorded on a WITec confocal Raman microscope CRM alpha 300 (Institute of Material Science, University of Silesia, Poland) equipped with an air-cooled solid-state laser emitting at 532 nm (green), and a CCD camera operating at −58 °C. Raman scattered light was focused onto a multi-mode fibre (50 μm diameter) and monochromator with 600/mm grating. The monochromator spectrometer was calibrated using the Raman scattering line of a silicon plate (520.7 cm^{-1}). Ten to fifteen scans with an integration time of 5–10 s each and a resolution of 3 cm^{-1} were collected and averaged.

Table 3 Parameters for X-ray data collection and structure refinement for chlorellestadite

Temperature, K	293(2)
Crystal data	
Crystal system	hexagonal
Unit cell dimensions (Å)	$a = 9.6002(2)$ $b = 9.6002(2)$ $c = 6.8692(2)$ $\alpha, \beta = 90°$ $\gamma = 120°$
Space group	$P6_3/m$ (no.176)
Volume ($Å^3$)	548.27(3)
Z	2
Density (calculated)	3.148 g/cm^3
Chemical formula	$Ca_{10}[(SiO_4)_3(SO_4)_3]Cl_{1.56}F0.34$
Crystal size (mm)	20×20×20 μm
Diffractometer super nova	
X-ray radiation	Mo$K\alpha$/0.71073 Å
X-ray power source	micro-focus sealed X-ray tube
Monochromator	Graphite
Max. θ°-range for Data collection	26.37
Index ranges	$-12 \le h \le 10$ $-11 \le k \le 12$ $-8 \le l \le 8$
No. of measured reflections	6993
No. of unique reflections	406
No. of observed reflections ($I > 2\sigma$ (I))	372
Refinement of the structure	
No. of parameters used in refinement	42
Rint	0.0303
Rσ	0.0093
R1. $I > 2\sigma$(I)	0.0356
R1 all Data	0.0388
wR2 on (F2)	0.0865
GooF	1.130
Δρ min (−e. Å-3) 0.80 Å from O2	−0.61
Δρ max (e. Å-3) 0.81 Å from O2	0.77

Occurrence and description of chlorellestadite

The altered xenolith of carbonate-silicate rock in which the chlorellestadite was found is enclosed in rhyodacite lava on the north-west slope of the Shadil-Khokh volcano, the Kel' volcanic plateau, Great Caucasus Mountain Range, Southern Ossetia (42°32′32.5″N, 44°17′50.7″E). This xenolith had been found in 2010 by V.G. and preliminary data on geological occurrence and mineral assemblage were published by Gazeev et al. (2012). The visible part of the xenolith is about 1.5 × 3 m in size and its interior is composed of coarse-grained brownish-grey marble. Along its periphery, the xenolith is more compact and consists of fine-grained skarn rock of variable color (Fig. 1; Galuskina et al. 2015). The thickness of the outer zone reaches about 20–30 cm, but the transition is gradual and indistinct. The same xenolith is also the type location for gazeevite, $BaCa_6(SiO_4)_2(SO_4)_2O$, which was simultaneously found in pyrometamorphic larnite rocks of the Hatrurim Complex in Israel (Galuskin et al. 2017). In addition, this is also the second known location of eltyubyuite, $Ca_{12}Fe_{10}Si_4O_{32}Cl_6$ (Gfeller et al. 2015), the rare Ca-humites kumtyubeite, $Ca_5(SiO_4)_2F_2$, and fluorchegemite, $Ca_7(SiO_4)_3F_2$ (Galuskina et al. 2015), as well as of dargaite, $BaCa_{12}(SiO_4)_4(SO_4)_2O_3$ (Galuskin et al. 2017).

Table 4 Atom coordinates and U^{iso} - equivalent isotropic displacement parameters (Å^2) for chlorellestadite

site	atom	x	y	z	U^{iso}	occ
S1	S	0.59645(13)	0.62679(13)	0.25	0.0145(3)	0.5
Si1	Si	0.59645(13)	0.62679(13)	0.25	0.0145(3)	0.5
Ca1	Ca	0.3333	0.6667	0.99749(19)	0.0312(4)	1
Ca2	Ca	0.25990(15)	0.25442(14)	0.25	0.0339(4)	1
O1	O	0.6657(5)	0.5124(5)	0.25	0.0308(9)	1
O2	O	0.0882(4)	0.3529(4)	0.4311(5)	0.0471(9)	1
O3	O	0.4113(4)	0.5344(4)	0.25	0.0337(10)	1
ClA	Cl	0	0	0.0517(14)	0.0351(12)	0.237(6)
ClB	Cl	0	0	0.142(3)	0.0351(12)	0.153(6)
F	F	0	0	0.25	0.0351(12)	0.175(16)

Ellestadite-group minerals are to be found throughout the skarn of the xenolith, but Cl-OH-bearing fluorellestadite is prevalent (Galuskina et al. 2015). F-OH-bearing chlorellestadite is confined to light fragments of spurrite rock with dark-green spots and light-brown zones along fractures (Fig. 1). Chlorellestadite as well as spurrite occur as rock-forming minerals (Fig. 2a). The former is extensively replaced by ettringite and a fine-grained mixture of minerals such as tobermorite, jennite, afwillite and unidentified hydrosilicates. Some fragments of rock are enriched with larnite relics, rondorfite grains and minerals of the wadalite-chlormayenite series and secondary hydrocalumite (Fig. 2b). Srebrodolskite, baryte, magnesioferrite-spinel series and periclase replaced by brucite are accessory minerals. Calcite is occasionally present. Green fragments of rock contain a considerable amount of oldhamite, replaced by ettringite, and minerals of the jasmundite-"alinite" series (Fig. 2c). "Alinite" is the chloride analogue of jasmundite known as a component of "green" cements, to which the formula $Ca_{10}Mg_{0.7}\square_{0.3}[(SiO_4)_{3.6}(AlO_4)_{0.4}]O_2Cl$ is attributed (Neubauer and Pöllmann 1994). In light-brown fragments, Fe-bearing wadalite and srebrodolskite are more commonly observed in the vicinity of fractures, in addition to grains of gazeevite, dargaite, rusinovite, eltyubyuite, "alinite", as well as potentially new minerals not formally approved by IMA-CNMNC with the compositions $Ca_3SiO_4Cl_2$ or $Ca_4Fe_2O_6Cl_2$ (Fig. 2d), here referred to as the anthropogenic phases "albovite" and "torbakovaite", respectively (Chesnokov et al. 1993a). That, unfortunately, "albovite" is unstable and disintegrates upon exposure to the atmosphere, and "torbakovaite" only forms very small grains up to 5 μm, has challenged reliable assessment of these phases.

Chlorellestadite forms inhomogeneous, porous, elongate grains up to 0.2-0.3 mm in length, partially replaced by secondary minerals, commonly represented by spherolitic aggregates (Fig. 2a, b). That the size of the single crystal fragment we were able to extract is below 30 μm, raises difficulties in the study of chlorellestadite.

In hand sample, chlorellestadite appears off-white with a bluish-greenish hue, and has a white streak and vitreous lustre. In thin section, chlorellestadite is colorless, transparent and not pleochroic. It shows no fluorescence in SW and LW ultraviolet illumination. Vickers nano-indentation hardness (n = 4, maximum load: 20.00mN) averages to VHN = 443, which is about 4–4.5 on the Mohs hardness scale, i.e., slightly harder than fluorite. Cleavage is indistinct parallel to elongation. No parting was observed though the mineral is brittle and shows an irregular fracture. Due to small size of the chlorellestadite crystals and the presence of

Table 5 Anisotropic displacement parameters (Å^2) for chlorellestadite

Atom	U^{11}	U^{22}	U^{33}	U^{23}	U^{13}	U^{12}
S1	0.0162(6)	0.0146(6)	0.0151(6)	0	0	0.0094(4)
Si1	0.0162(6)	0.0146(6)	0.0151(6)	0	0	0.0094(4)
Ca1	0.0398(5)	0.0398(5)	0.0140(6)	0	0	0.0199(3)
Ca2	0.0399(7)	0.0353(7)	0.0215(6)	0	0	0.0151(5)
O1	0.048(2)	0.034(2)	0.0226(18)	0	0	0.0295(19)
O2	0.0343(15)	0.074(2)	0.0417(18)	0.0336(17)	0.0161(14)	0.0336(15)
O3	0.0236(18)	0.0234(18)	0.053(3)	0	0	0.0109(16)

Table 6 Selected interatomic distances (Å) in chlorellestadite

S1/Si1	O2	1.537(3)	×2
	O3	1.540(4)	
	O1	1.543(4)	
	mean	1.539	
Ca1	O1	2.421(3)	×3
	O3	2.476(3)	×3
	O2	2.786(4)	×3
	mean	2.561	
Ca2	O3	2.330(4)	
	O2	2.349(3)	×2
	O2	2.592(3)	×2
	O1	2.800(4)	
	mean	2.503	
Ca2	ClA	2.820(5)	×2
	ClB	2.578(6)	×2
	F	2.4692(12)	

larnite, spurrite and other inclusions, density could not be measured. Instead, density was calculated from the empirical crystal chemical formula and unit-cell volume and gives the value 3.091 g/cm^3, similar to the density of other Ca-members of the ellestadite group.

The chemical composition of chlorellestadite shows little variation (Table 2). The empirical formula based on 8 cations plus

Fig. 1 Type specimen containing chlorellestadite. For description of zonation, see text

hydrous species and assuming charge balance is calculated as: $Ca_{4.99}Na_{0.01}(SiO_4)_{1.51}(SO_4)_{1.46}(PO_4)_{0.03}(Cl_{0.61}OH_{0.21}F_{0.11})_{\Sigma 0.93}$, which can be idealized as $Ca_5(SiO_4)_{1.5}(SO_4)_{1.5}Cl$. The slight deficiency of sulphur in the empirical crystal chemical formula of chlorellestadite may be attributed to the presence of minor CO_3 in the tetrahedral site, which seems confirmed by Raman spectroscopy (see Fig. 5b). In 2016, a CO_3-bearing member of the hydroxylellestadite-hydroxylapatite series was described from Tadano, Japan (Banno et al. 2016). The small charge deficiency of channel anions (Cl, OH, F) is compensated by an excess in tetrahedral anions (SiO_4^{4-}, PO_4^{3-}).

Structure of chlorellestadite

The crystal structure of natural chlorellestadite is nearly identical to that of its synthetic analogues. Differences are observed only in anion channel sites (Fang et al. 2011, 2014). Unit-cell parameters of the natural chlorellestadite described here ($P6_3/m$, $a = 9.6002(2)$, $c = 6.8692(2)$ Å, $V = 548.27(3)$Å^3) are closest to the synthetic analogue with the composition $Ca_5[(SiO_4)_{0.5}(SO4)_{0.5}]Cl_{0.8}F_{0.2}$ ($P6_3/m$, $a = 9.6239$ (3), $c = 6.87749$ (3), Å, $V = 551.64(3)$ Å^3) (Fang et al. 2011). The topology of the chlorellestadite structure (apatite supergroup, Pasero et al. 2010) can be presented as consisting of a $Ca_4[(S,Si)O_4]_6$ framework with channels along the c axis, containing columns of $Ca_6[Cl,F,(OH)]_2$ (Fig. 3a). The anion sites in the centre of channels with coordinates (0,0,z): ClA ($z = 0.05$), ClB ($z = 0.14$) and F($z = 0.25$) (Fig. 3b), are only partially occupied, refined to 0.24 (0.48 Cl pfu), 0.15 (0.30 Cl pfu) and 0.17 (0.17 F pfu), respectively (Table 4). Positions of Cl and F atoms in channels are more similar to anion positions in fluorapatite with composition $Ca_5(PO_4)_3(F_{0.39}Cl_{0.33}OH_{0.28})$ ($P6_3/m$, $a = 9.459(2)$, $c = 6.849(2)$, Å, V = 530.987 Å^3): ClA ($z = 0.06$), ClB ($z = 0.13$), F ($z = 0.25$) and (OH) ($z = 0.30$) (Hughes et al. 1990). In chlorapatite with composition ~$Ca_5(PO_4)_3[Cl_{0.85}(OH_{0.15})]$, the ClA site occurs at $z = 0.06$, ClB – at $z = 0.10$ and (OH) – at $z = 0.18$ (Hughes et al. 2016). In synthetic chlorellestadite, the Cl position occurs at z = 0.07 and splitting of Cl over two sites seems absent (Fang et al. 2014). In the studied chlorellestadite, there are distances: Ca2-ClA = 2.82 Å, Ca2 – ClB = 2.58 Å and Ca2 – F = 2.50 Å (Fig. 3b; Table 6). The distance between Ca2 and ClB is shorter in comparison with typical Ca-Cl distances (Kelly et al. 2017), which seems to imply mixed occupation Cl + OH(F) of this site. Probably, the presence of Cl at the ClB site is balanced by splitting of the Ca2 site, which is known for chlorapatite (Hughes et al. 2016; Kelly et al. 2017). However, this type of site splitting was not observed in the chlorellestadite from South Ossetia. Calculation of channel site occupation with regard to electronic density, channel anion sum = 1 pfu and mixed character of ClB site occupation gives a structural formula with relatively higher Cl content -

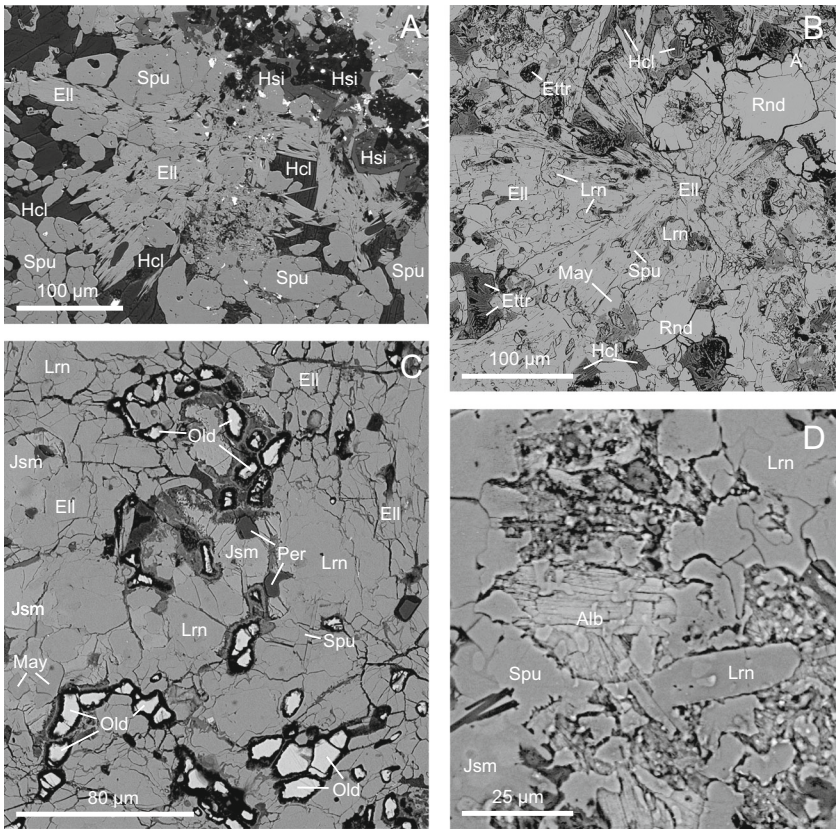

Fig. 2 Chlorelletadite and associated minerals in dark-green (**a**, **c**) and light (**b**, **d**) zones of host rock. BSE images. Alb – albovite, Els – chlorellestadite, Ettr – ettringite, Hcl – hydrocalumite, Hsi – unidentified Ca-Al-Mg - hydrosilicates, Jsm – jasmundite, Lrn – larnite, May – chlormayenite, Old – oldhamite, Per – periclase, Rnd – rondorfite, Sbr – srebrodolskite, Spu – spurrite

$Ca_5(SiO_4)_{1.5}(SO_4)_{1.5}Cl_{0.74}(OH,F)_{0.26}$, in comparison with the empirical formula - $(Ca_{4.98}Na_{0.01})_{\Sigma 4.99}[(SiO_4)_{1.51}(SO_4)_{1.47}(PO_4)_{0.03}]_{\Sigma 3.01}(Cl_{0.61}OH_{0.28}F_{0.11})_{\Sigma 1.00}$. Interestingly, the refinement of the chlorellestadite structure using anisotropic displacement parameters (this solution was used in the check-list for new mineral) for all atoms allowed definition of only Cl positions in channels: ClA ($z = 0.07$) and ClB ($z = 0.19$), which gave the structural formula $Ca_5(SiO_4)_{1.5}(SO_4)_{1.5}Cl_{0.59}(OH,F)_{0.41}$, which is closer to the empirical formula (Table 2). Higher Cl contents in the structural formula of chlorellestadite can be ascribed to both high crystal inhomogeneity and artefacts caused by small size of the studied crystal. The fragment of chlorellestadite crystal for structural study was extracted from a small spherolithic aggregate ~60 × 120 μm in size, on which 11 microprobe analyses were performed using a broader beam to minimize S loss (Table 2). It is possible that part of Cl was also lost (Cazaux 1996; Stromer et al. 1993).

A sequence of channel site occupation preserving symmetry based on ratio of site occupation and real interatomic distances is shown in Fig. 4. It is similar in Cl-dominant apatites, which display a splitting of the Cl site (Hughes et al. 2014a, b, 2016). In the synthetic chlorapatite-chlorellestadite series, a splitting of the Cl site is observed only in chlorapatite (Fang et al. 2014). The ClA-ClB distance is 2.81 Å in the studied chlorellestadite (Fig. 4) is shorter than the typical Cl-Cl distance of ~3-4Å (Vener et al. 2013), which confirms our assumption about mixed Cl + OH(F) occupation of the ClB site.

There exists the following structural data for the ellestadite group minerals: hydroxylellestadite from Cioclovina Cave, Romania ($P6_3/m$, $a = 9.496(2)$, $c = 6.920(2)$ Å, $V = 540.4$ Å^3; Onac et al. 2006); Crestmore, California, USA ($P2_1/m$, $a = 9.5224$, $b = 9.5268$, $c = 6.9087$ Å, $\beta = 119.9483°$, $V = 531.48$ Å^3; Hughes and Drexler 1991) and Chichibu, Japan ($P2_1/m$, $a = 9.476(2)$, $b = 9.508(2)$, $c = 6.919(1)$ Å, $\beta = 119.53°$, $V = 542.41$ Å^3; Sudarsanan 1980). The symmetry reduction of hydroxylellestadite relates to F, Cl and (OH) ordering in channel sites as well as cation ordering in tetrahedral sites (Sudarsanan 1980; Hughes and Drexler 1991). Our structural data does not allow any statement about symmetry reduction of the chlorellestadite from Southern Ossetia.

Recently, a mineral of the hydroxylapatite-hydroxylellestadite series with a high CO_3 content was described by Banno et al. (2016). This points to the possibility of finding a CO_3-analogue of hydroxylellestadite $Ca_5(SiO_4)_{1.5}[(CO_3),(SO_4)]_{1.5}(OH,Cl,F)$. In the Raman spectrum of chlorellestadite, the band at 1078 cm^{-1} can be an overlaying of $\nu_3(SO_4)$ and $\nu_1(CO_3)$. We cannot exclude a negligible amount of CO_3 in the composition of chlorellestadite, but that does not change the common crystal chemical interpretation.

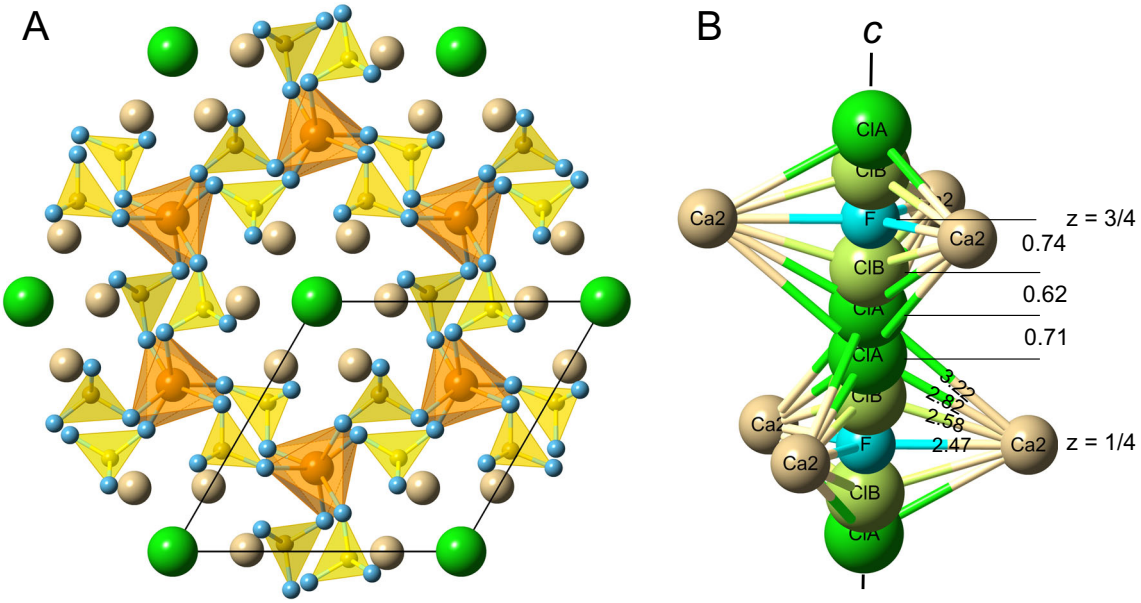

Fig. 3 **a** – chorellestadite atomic arrangement projected on (001). Green atoms represent projection of anion column, yellow atoms are S and Si, brown atoms are Ca1 and tan atoms are Ca2. **b** – anion column within the one unit-cell

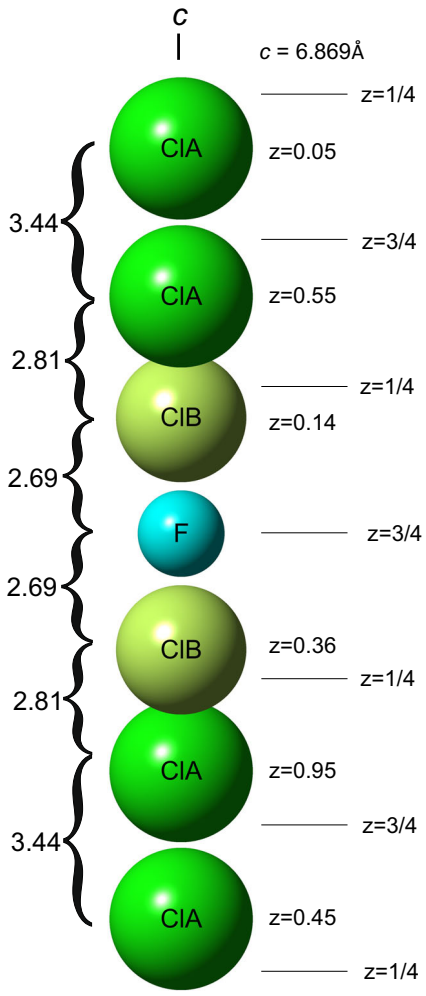

Fig. 4 Depiction of reversal anion column in chlorellestadite from Shadil Khokh volcano. All distances are given in Å

Raman spectroscopy of chlorellestadite

The Raman spectrum of holotype chlorellestadite (Fig. 5) is analogous to other spectra of the ellestadite group minerals (Harada et al. 1971; Livingstone et al. 1987; Onac et al. 2006). The main bands correspond to the Si-O and S-O vibrations in tetrahedral sites. The spectrum of chlorellestadite can be divided into two regions: 150–700 cm^{-1} (a) and (b) 700–1200 cm^{-1}.

The first region (a) is characterized by the appearance of many overlapping bands marked by low-intensity. Relatively intense bands at 649 and 630 cm^{-1} are in this range; they correspond to the ν_4 bending vibrations connected with the SO_4^{2-} group (Onac et al. 2006). Two lower intense bands at 536 and 572 cm^{-1} are related to the ν_4 vibrations caused by SiO_4^{4-} groups (Onac et al. 2006). Between 500 and 350 cm^{-1} a variety of small bands can be observed. This is an effect of the mutual influence on crystal structure of SO_4^{2-} and SiO_4^{4-} groups in tetrahedral sites. These are mainly ν_2 bending vibrations of SO_4^{2-} and SiO_4^{4-} (Frost et al. 2007; Frost and Palmer 2011) and additional bands connected to vibrations of Ca–O–Ca and O–Ca–O groups. Below 350 cm^{-1}, broad bands correspond to translation moves of atoms and rotational motions of entire molecules. Three relatively intense bands occurring at 311, 267 and 230 cm^{-1} may be caused by translation moves of O–Ca–O (Dulski et al. 2013) as well as by rotation of SO_4^{2-} and SiO_4^{4-} groups (Frost et al. 2007; Frost and Palmer 2011). Furthermore, Frost suggests that weak bands located in the 200–150 cm^{-1} range relate to the Cl–M–Cl bending mode, where M = Ca (Frost and Keeffe 2009).

In the second region (b), only a few bands of stronger intensity appear. The two most intense bands are located at

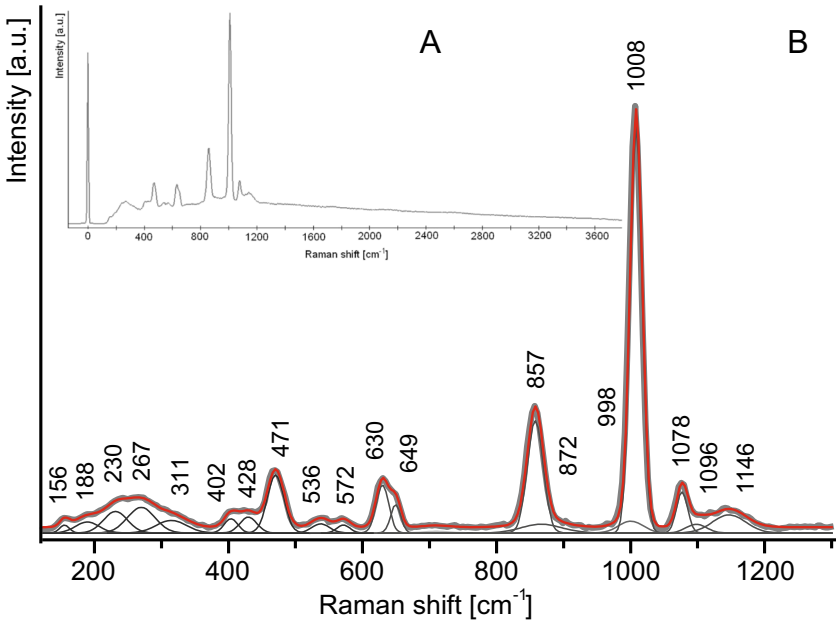

Fig. 5 Raman spectrum of chlorellestadite: **a** – full spectrum in the 100–3800 cm^{-1} range; **b** – peak-fitted spectrum in the 100–1300 cm^{-1} region. Thick grey line – original spectrum. Thick-red line – fitted spectrum. Thin dark-grey line – peaks

1008 and 857 cm^{-1} and connected to the ν_1 symmetric vibrations of the SO_4^{2-} and SiO_4^{4-}, respectively (Arkhipenko and Moroz 1997; Comodi et al. 2016). Weak bands occurring in the 1070–1150 cm^{-1} region correspond to the combination of ν_3 antisymmetric stretching vibrations of SiO_4 and SO_4 groups (Comodi et al. 2016). Presumably, ν_1 vibrations of CO_3 groups have a share in the band at 1078 cm^{-1} (Banno et al. 2016), but CO_3-group content is insignificant and was not taken into consideration in the calculation of the chlorellestadite crystal chemical formula.

Both spectra of F-Cl-bearing hydroxylellestadite and OH-Cl-bearing fluorellestadite from the xenolith from the Shadil-Khokh volcano have bands in the 3500–3600 cm^{-1} range related to the presence of a hydroxyl group in the channel sites (Onac et al. 2006; Comodi et al. 2016). In this range, the fact that the chlorellestadite spectrum does not show bands reflects the low water content in the chemical composition of the studied fragment of the mineral. Probably, the relatively large and heavy Cl prevailing in the structural channel influences the character of the OH group vibrations.

Discussion

In the preliminary study of the Shadil Khokh xenolith, Gazeev et al. (2012) listed only rondorfite and secondary-phase hydrocalumite as Cl-bearing minerals components (Gazeev et al. 2012). Later, eltyubyuite and rusinovite were described in cuspidine-bearing veins together with hydrocalumite (Gfeller et al. 2015). Our investigations revealed a considerably greater number of Cl-bearing minerals in the xenolith, namely, chlorellestadite, the chlorine analogue of jasmundite, chlormayenite-wadalite series, "albovite" and "torbakovaite". "Albovite" and "torbakovaite" were described by Chesnokov et al. in 1993 and who associated their formation with the high-temperature alteration of carbonatized wood in a Cl-bearing environment in burnt coal heaps (Chesnokov et al. 1993a, b, 2008). It should be noted that the potentially new mineral "albovite", $Ca_3(SiO_4)Cl_2$, found in the mineral association of the Shadil Khokh volcano, is the natural chlorosilicate with the highest chlorine content. Its chemical composition is as follows (wt%): Ca 42.25, Si 10.52, Cl 23.72 (our data and Chesnokov et al. 2008).

The external part of the xenolith and the thin endoskarn zone (up to 1 cm) developed after the volcanic rock was enriched in chlorine. Some samples from the near-contact part of the xenolith exhibit well-defined zoning: dark zones with Mg-bearing minerals such as merwinite, bredigite, rondorfite, spinel-magnesioferrite and light zones with predominant Ca-minerals – spurrite, minerals of the ellestadite series and Ca-humites (Galuskina et al. 2015). In both zone types, varying amounts of larnite, minerals of the chlormayenite-wadalte series and srebrodolskite are also present. Calcite marble occurs in internal part of the xenolith. It is assumed that this relatively large xenolith originated from the walls of the volcanic neck and, for some time before it was moved in lava to the surface, was in an area most exposed to volcanic gases. The process of xenolith alteration likely began with the recrystallization of the carbonate-silicate protolith and the formation of minerals in contact with hot lava. Volume change and fracture development associated with this early stage, in turn, aided intensive processing of near-contact parts of xenolith by volcanic gases and fluids. Minerals with high chlorine contents such as rusinovite (Cl ~ 7 wt%), "albovite" (Cl ~ 24 wt%), "torbakovaite" (Cl ~ 16 wt%) and eltybyuite (Cl ~ 10 wt%) developed in the vicinity of fractures mainly whereas, in the

groundmass of rock, chlorine occurs in minerals of the ellestadite (up to Cl ~ 5 wt%), of the chlormayenite-wadalite (Cl ~ 4–6 wt%) series and in rondorfite (Cl ~ 7 wt%).

Volcanic exhalations are the most probable source of chlorine in the xenolith minerals. Chlorine is a common constituent of volcanic gases and aqueous intrusions (Kuroda and Sandell 1953; Yoshida et al. 1971; Kanazawa et al. 1997). Hydrogen chloride formed at high temperatures by the reaction $Cl^- + H_2O \leftrightarrow HCl + OH^-$ (Kuroda and Sandell 1953) is one of the four most common constituents of high-temperature volcanic emissions; the others are H_2O, CO_2 and sulphur compounds (Pyle and Mather 2009). Chlorides separate out and are released from ascending magma at relatively shallow depths due to pressure loss and melt crystallization as the magma ascends in the vent and erupts (Aiuppa et al. 2009; Chevychelov et al. 2008).

The temperature of chlorellestadite genesis can be comparable to that of synthetic chlorellestadite which forms at 965–1165 °C (von Lampe et al. 1989; Saint-Jean and Hansen 2005). That temperature also corresponds to the temperature of wadalite formation (Kanazawa et al. 1997), which occurs associated with chlorellestadite.

Acknowledgements This work was supported by grant no. 2015/17/N/ST10/03141 (D. Ś.) from the National Science Centre (NCN) of Poland. Professor Pádhraig S. Kennan of University College at Dublin, Ireland, kindly helped with the English language. The authors are grateful to referee Professor S. Mills and Editor-in-Chief Dr. M.A.T.M. Broekmans for their constructive remarks, which greatly improved the original manuscript.

References

Aiuppa A, Baker DR, Webster JD (2009) Halogens in volcanic systems. Chem Geol 263:1–18

Arkhipenko D, Moroz T (1997) Vibration spectrum of natural ellestadite. Crystallogr Rep 42:651–656

Banno Y, Miyawaki R, Momma K, Bunno M (2016) A CO_3-bearing member of the hydroxylapatite-hydroxylellestadite series from Tadano, Fukushima prefecture, Japan: CO_3-SO_4 substitution in the apatite-ellestadite series. Mineral Mag 80:363–370

Cazaux J (1996) Electron probe microanalysis of insulating materials: quantification problems and some possible solutions. X-Ray Spectrom 25:265–280

Chen M, Fang Y (1989) The chemical composition and crystal parameters of calcium chlorosulfatosilicate. Cem Concr Res 19:184–188

Chesnokov B, Bazhenova LF, Bushmakin AF (1987) Fluorellestadite Ca10[(SO4),(SiO4)]6F2: A New Mineral Species. Zapiski Vsesouyuznogo Mineralogicheskogo Obshchestva/RU 116:743–746

Chesnokov B, Bazhenova L, Bushmakin A, Vilisov V, Kretser Y, Nishanbaev T (1993a) New minerals of burned spoil-heaps of the Chelyabinsk coal basin (communication no. 4). In: Ural mineralogical volume. UIF "Nauka," Ekaterinburg/RU, pp 3–25

Chesnokov B, Vilisov V, Bazhenova L, Bushmakin, AF, Kotlyarov VA (1993b) New minerals of burned spoil-heaps of the Chelyabinsk coal basin (communication no. 5). In: Ural mineralogical volume. UIF "Nauka," Ekaterinburg/RU, pp 3–36

Chesnokov B, Shcherbakova E, Nishanbaev T (2008) Minerals of burned spoil-heaps of the Chelyabinsk coal basin. IMin UrO RAS, Miass/RU

Chevychelov V, Botchamikov R, Holtz F (2008) Partitioning of cl and F between fluid and hydrous phonolic melt of Mt. Vesuvius at 850-1000°C and 200 MPa. Chem Geol 256:172–184

Comodi P, Liu Y, Stoppa F, Woolley AR (2016) A multi-method analysis of Si^-, S^- and REE-rich apatite from a new find of kalsilite-bearing leucitite (Abruzzi, Italy). Mineral Mag 63:661–672

Dulski M, Bulou A, Marzec KM, Galuskin EV, Wrzalik R (2013) Structural characterization of rondorfite, calcium silica chlorine mineral containing magnesium in tetrahedral position $[MgO_4]^{6-}$, with the aid of the vibrational spectroscopies and fluorescence. Spectrochim Acta A Mol Biomol Spectrosc 101:382–388

Fang Y, Ritter C, White T (2011) The crystal chemistry of $Ca_{10-y}(SiO_4)_3(SO_4)_3Cl_{2-x-2y}F_x$ ellestadite. Inorg Chem 50:12641–12650

Fang YN, Ritter C, White TJ (2014) Crystal chemical characteristics of ellestadite-type apatite: implications for toxic metal immobilization. Dalton Trans 43:16031–16043

Frost RL, Keeffe EC (2009) Raman spectroscopic study of the selenite mineral mandarinoite $Fe_2Se_3O_9{\cdot}6H_2O$. J Raman Spectrosc 40:42–45

Frost RL, Palmer SJ (2011) Raman spectroscopic study of the minerals diadochite and destinezite $Fe^{3+}{}_2(PO_4,SO_4)_2(OH){\cdot}6H_2O$: implications for soil science. J Raman Spectrosc 42:1589–1595

Frost RL, Palmer SJ, Bouzaid JM, Reddy BJ (2007) A Raman spectroscopic study of humite minerals. J Raman Spectrosc 38:68–77

Galuskin EV, Gfeller F, Galuskina IO, Armbruster T, Krzątała A, Vapnik Y, Kusz J, Dulski M, Gardocki M, Gurbanov AG, Dzierżanowski P, Gatta GD (2017) New minerals with a modular structure derived from hatrurite from the pyrometamorphic rocks. Part III. Gazeevite, $BaCa_6(SiO_4)_2(SO_4)_2O$, from Israel and the Palestine autonomy, South Levant, and from South Ossetia, greater Caucasus. Mineral Mag 81:499–513

Galuskina IO, Krüger B, Galuskin EV, Armbruster T, Gazeev VM, Włodyka R, Dulski M, Dzierżanowski P (2015) Fluorchegemite, $Ca_7(SiO_4)_3F_2$, a new mineral from the edgrewite-bearing endoskarn zone of an altered xenolith in ignimbrites from upper Chegem caldera, northern Caucasus, Kabardino-Balkaria, Russia: occurrence, crystal structure, and new data on the mineral assemblages. Can Mineral 53:325–344

Gazeev VM, Gurbanova O, Zadov AE, Gurbanov AG, Leksin, AB (2012) Mineralogy of skarned carbonate xenoliths from Shadil-Khokh volcano – (Kelski Vulcan area of Great Caucasian Range) (in Russian) Vestnik Vladikavkazskogo Nauchnogo Cent 2:18–27

Gfeller F, Środek D, Kusz J, Dulski M, Gazeev V, Galuskina I, Galuskin E, Armbruster T (2015) Mayenite supergroup, part IV: crystal structure and Raman investigation of Al-free eltyubyuite from the Shadil-Khokh volcano, Kel' plateau, southern Ossetia, Russia. Eur J Mineral 27:137–143

Harada K, Hagashima K, Nakao K, Kato A (1971) Hydroxylellestadite, a new apatite from Chichibu mine, Saitama prefecture, Japan. Am Mineral 56:1507–1518

Hughes J, Drexler J (1991) Cation substitution in the apatite tetrahedral site: crystal structures of type hydroxylellestadtite and type fermorite. Neues Jahrb Mineral Monatshefte 1991(7):327–336

Hughes J, Cameron M, Crowley K (1990) Crystal structures of natural ternary apatites: solid solution in the $Ca_5(PO_4)_{3X}$ (X = F, OH, Cl) system. Am Mineral 75:295–304

Hughes JM, Heffernan KM, Goldoff B, Nekvasil H (2014a) Cl-rich fluorapatite, devoid of OH, from the Three Peaks Area, Utah: The first reported structure of natural Cl-rich fluorapatite. Can Mineral 54(4):643–652

Hughes JM, Nekvasil H, Ustunisik G, Lindsley DH, Coraor AE, Vaughn J, Phillips BL, McCubbin FM, Woerner WR (2014b) Solid solution in the fluorapatite-chlorapatite binary system: high-precision crystal structure refinements of synthetic F-cl apatite. Am Mineral 99:369–376

Hughes JM, Harlov D, Kelly SR, Rakovan J, Wilke M (2016) Solid solution in the apatite OH-cl binary system: compositional dependence of solid-solution mechanisms in calcium phosphate apatites along the cl-OH binary. Am Mineral 101:1783–1791

Kanazawa Y, Aoki M, Takeda H (1997) Wadalite, rustumite and spurrite from La Negra mine, Queretaro, Mexico. Bull Geol Surv Jpn 48: 413–420

Kelly SR, Rakovan J, Hughes JM (2017) Column anion arrangements in chemically zoned ternary chlorapatite and fluorapatite from Kurokura, Japan. Am Mineral 102:720–727

Kuroda PK, Sandell EB (1953) Chlorine in igneous rocks – some aspects of the geochemistry of chlorine. GSA Bull 64:879–896

Le Roy AF, Roinel N (1983) Radiation damage to lyophilized mineral solutions during electron probe analysis: quantitative study of chlorine loss as a function of beam current-density and sample mass-thickness. J Microsc 131:97–106

Livingstone A, Ryback G, Fejer EE, Stanley CJ (1987) Mattheddleite, a new mineral of the apatite group from Leadhills, Strathclyde region. Scott J Geol 23:1–8

McConnell D (1937) The substitution of SiO_4- and SO_4-groups for PO_4-groups in the apatite structure; ellestadite, the end-member. Am Mineral 22:977–986

Morgan GB, London D (1996) Optimizing the electron microprobe analysis of hydrous alkali aluminosilicate glasses. Am Mineral 81:1176–1185

Neubauer J, Pöllmann H (1994) Alinite – chemical composition, solid solution and hydration behaviour. Cem Concr Res 24:1413–1422

Onac BP, Effenberger H, Ettinger K, Panzaru SC (2006) Hydroxylellestadite from Cioclovina cave (Romania): microanalytical, structural, and vibrational spectroscopy data. Am Mineral 91: 1927–1931

Pasero M, Kampf AR, Ferraris C, Pekov IV, Rakovan J, White TJ (2010) Nomenclature of the apatite supergroup minerals. Eur J Mineral 22: 163–179

Pliego-Cuervo YB, Glasser FP (1977) The role of sulphates in cement clinkering reactions: phase formation and melting in the system CaO-Ca_2SiO_4-$CaSO_4$-K_2SO_4. Cem Concr Res 7:477–481

Pouchou JL, Pichoir F (1985) "PAP" phi-rho-Z procedure for improved quantitative microanalysis. In: Armstrong JT (ed) Microbeam analysis. San Francisco Press, San Francisco, pp 104–106

Pyle DM, Mather TA (2009) Halogens in igneous processes and their fluxes to the atmosphere and oceans from volcanic activity: a review. Chem Geol 263:110–121

Rouse R, Dunn P (1982) A contribution to the crystal chemistry of ellestadite and the silicate sulfate apatites. Am Mineral 67:90–96

Saint-Jean SJ, Hansen S (2005) Nonstoichiometry in chlorellestadite. Solid State Sci 7:97–102

Sejkora J, Houzar S, Srein V (1999) Clorem Bohaty Hydroxyellestadit ze Zastavky u Brna. Acta Musei Morav 84:49–59

Sheldrick GM (2015) Crystal structure refinement with SHELXL. Acta Crystallogr Sect C Struct Chem 71:3–8

Stromer J, Milton L, Pierson L, Tacker R (1993) Variation of F and cl X-ray intensity due to anisotropic diffusion in apatite during electron microprobe analysis. Am Mineral 78:641–648

Sudarsanan K (1980) Structure of hydroxylellestadite. Acta Crystallogr B 36:1636–1639

Vener MV, Shishkina AV, Rykounov AA, Tsirelson VG (2013) Cl···cl interactions in molecular crystals: insights from the theoretical charge density analysis. J Phys Chem A 117:8459–8467

von Lampe F, Grimmer A-R, Wallis B (1989) Preparation and characterization of the calcium silicate sulfate chloride $Ca_4(SiO_4)(SO_4)Cl_2$. Cem Concr Res 19:595–602

Whitney DL, Evans BW (2010) Abbreviations for names of rock-forming minerals. Am Mineral 95:185–187

Yoshida M, Takahashi K, Norinobu Y, Takejiro O, Iwaji I (1971) The fluorine, chlorine, bromine and iodine contents of volcanic rocks in Japan. Bull Chem Soc Jpn 44:1844–1850